Visualization and Analysis of Myocardial Transition by Cardiac Ultrasound Images

Naohiro AMAMOTO, Osamu OSHIRO, Ayumu MATANI,
Kosuke SATO and Kunihiro CHIHARA

Graduate School of Information Science, Nara Institute of Science and Technology.

1 Introduction

Echocardiography is a technique widely used for the anatomical diagnosis of most cardiac disorders because of its noninvasive and real-time observation. However, echocardiography is not suitable for functional diagnosis. Hence several investigations reported quantitative analysis using digital two-dimensional echocardiography.

Masuda et al.[1] proposed the technique which visualize instantaneous velocity of internal organs used subtraction of two echograms. Yamazaki et al.[2] proposed the technique to determine tissue motion with the utilization of color Doppler system as well. The problem with both of these techniques is that they are very sensitive to the noise. Mailloux et al.[3] reported a completely automated method to quantify the motion of heart based on computation of the optical flow. However, the computation of the optical flow is quite complex and requires such a long time that the advantage of echocardiography, the real-time process, is lost.

In this paper, we present the technique that extracts the tissue portion, the endocardial boundaries and the landmarks, and that tracks the cardiac wall motion using correspondence analysis of landmarks between successive two echograms. This technique allows us to visualize the movement and velocity of the endocardial boundaries. We also indicate the evaluated result about the accuracy of segmentation and tracking technique.

2 Segmentation and detection of landmarks

2.1 Segmentation of echocardiogram

It is important to segment the echocardiogram into the image of cardiac organs and the background image to evaluate for quantitive evaluation. Muzzolini et al.[4] indicated the segmentation method of ultrasound images which generalized the conventional simulated annealing method to a multiresolution framework and minimized an energy function. However, this technique is complex and consumes a large amount of time. Then, to extract the portion of cardiac organs from original image with little effect of noise, we carried out the region segmentation using the gradient relaxation method[5]. This technique is that the obscurity of the image is reduced in order to decrease the local contradiction. In [5], the initial value, called initial label probability, for segmentation are calculated by following equation.

$$P_i(\lambda_1) = \beta\frac{f_i - f_m}{G-1} + 0.5 \tag{1}$$

$$P_i(\lambda_2) = 1 - P_i(\lambda_1) \tag{2}$$

In above equation β is an appropriate constant(in general 0.7 - 1.0), f_m is average gray value of a whole image, G is the number of gray levels of a whole image and f_i is gray value of an object pixel. A set of N pixels $i = 1, 2, \cdots, N$ fall into two classes λ_1 and λ_2 corresponding to the white(gray value = 255) and the black(gray value = 0). However, it is difficult to segment the object and background accurately, if the above equation is applied to calculate the initial label probability. The reason is that most of pixels which comprise the ultrasound image, especially the echocardiogram(Fig.1(a)), have a most low gray level and consequently the average gray level of the image becomes very small. Therefore, we propose the method that the image is divided into some small portion and the initial value is calculated in each division image.

$$P_i(\lambda_1) = (1.0 - \frac{f_{a,j}}{f_{max}}) \times \frac{f_i - f_{a,j}}{G_j - 1} + 0.5 \tag{3}$$

$$P_i(\lambda_2) = 1 - P_i(\lambda_1) \tag{4}$$

where $f_{a,j}$ is average gray value of each division image, G_j is the number of gray levels of the whole image, f_{max} is the highest gray value in each division image and f_i is gray value of an object pixel. In above equation, if the $f_{a,j}$ and f_{max} are about the same value, then it seems that the division image is organized with homogeneous area. Otherwise, the division image seems to contain the background and the object. Therefore in the former case the weighted value$(1.0 - f_{a,j}/f_{max})$ becomes small, and the latter becomes large to make clear the background and the object. After calculation of the initial label probability using equation(3), (4), the label probability is updated by equation(5).

$$P_i^{new}(\lambda_k) = P_i^{old}(\lambda_k) + \rho_i(2Q_i(\lambda_k) - 1) \tag{5}$$

where ρ_i is a positive step size and is given by

$$\rho_i = \begin{cases} \alpha_1 \frac{1 - P_i^{old}(\lambda_1)}{2Q_i(\lambda_1) - 1} & 2Q_i(\lambda_1) - 1 > 0 \\ \alpha_2 \frac{P_i^{old}(\lambda_1)}{1 - 2Q_i(\lambda_1)} & 2Q_i(\lambda_1) - 1 < 0 \end{cases} \tag{6}$$

α_1, α_2 are positive constants less than unity and Q_i is defined as

$$Q_i(\lambda_k) = \frac{1}{8}\sum_{j=1}^{8} P_j(\lambda_k) \tag{7}$$

In above equation, $P_j(\lambda_k)$ is the label probability of the eight nearest pixels adjacent to the object pixel.

After updating with the suitable iteration, the gray value of each pixel are given by

$$f_i = P_i(\lambda_1)(G-1) \tag{8}$$

Fig.1(b) shows the segment result obtained from calculation of the initial value using equation(3), (4) and iteration of updating label probabilities five times. The endocardial boundary locations can be obtained by transforming this image into binary image and detecting the contour. Fig.1(c) is an image superimposed the endocardial boundary on a original B-mode image.

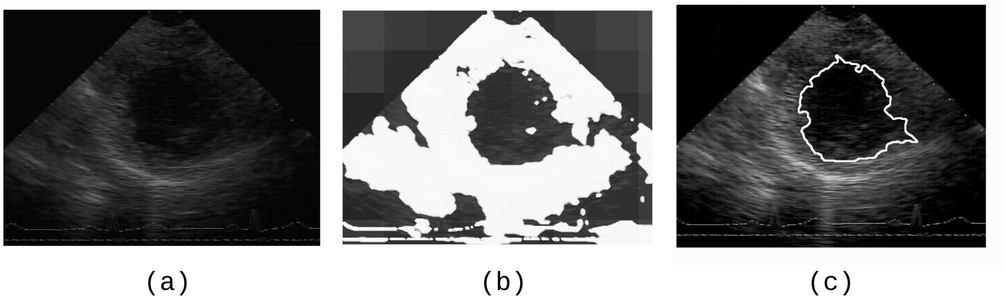
(a) (b) (c)

Figure 1: An example of applying our technique. (a)An ultrasound image at a systolic phase in a short axis view, (b)A result of segmentation, (c)An image superimposed detected edges from (b) on (a).

2.2 Detection of landmarks

From the result obtained by the process as mentioned above, the landmarks are determined by using geometric features. First, the endocardial boundaries are divided into four line-segment types using the masks shown in Fig.2. Next, landmarks are set of contact points between line-segments of different types. For a long line-segment, landmarks are placed on such segment at regular intervals.

0	0	0
1	1	1
0	0	0

0	1	0
0	1	0
0	1	0

1	0	0
0	1	0
0	0	1

0	0	1
0	1	0
1	0	0

Figure 2: The masks for detecting four types line-segments from endocardial boundaries.

3 Correspondence analysis of landmarks

To analyze the myocardial motion, landmarks are corresponded between successive two frames. Yachida[6] indicated the method which used velocity estimates of the prominent feature points as reliable initial estimates and propagated them to other points using a constraint relation between neighbouring points, on the assumption that the objects are rigid and their motion is smooth. However, the myocardium changes its shape and its motion is complex. Then we correspond the landmarks of the last frame to that of the current frame using the direction of the endocardial boundary and the distance between landmarks. Direction of the endocardial boundary on a landmark are assigned to the eight-directions by the Robinson's Edge Detector[7].

Comparing the directions of the endocardial boundary on the landmarks between two echocardiograms, all landmarks whose direction difference in angle within 45degrees are nominated for the corresponding point to allow varying myocardial shape. Among these points, the landmark nearest to the preceding image's landmark is determined as the corresponding point. A corresponding point of every landmarks on preceding image is obtained from the process.

In Fig.3, empty circles are landmarks and each arrow shows a direction of boundary. Landmarks P1, P2 and P3 in a current frame are nominated for corresponding point of a landmark P in the last frame. The landmark P3 is the nearest to P, then P3 is determined the corresponding point of P.

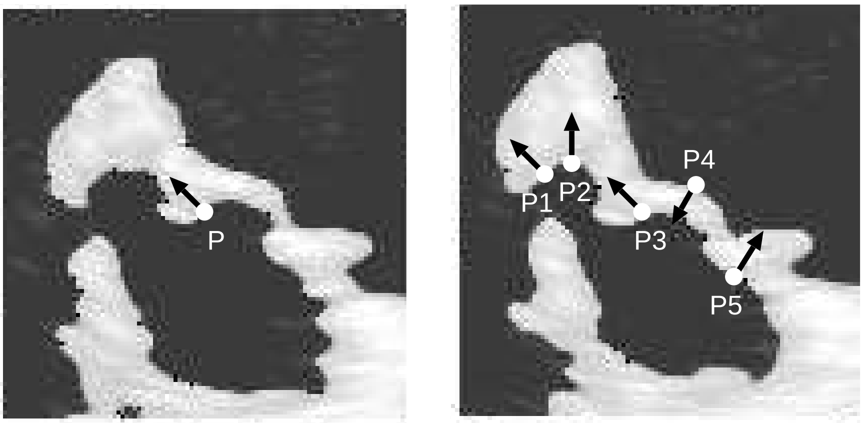

(a) (b)

Figure 3: An example of determining corresponding point.

4 Testing the algorithm

This section details the experimental method to evaluate the accuracy of the segmentation and the correspondence analysis and discusses the results obtained from these process.

4.1 Accuracy of segmentation

To evaluate the accuracy of the segmentation algorithm, the image of meat cube cut off 35mm and fixed in a water tank was used (Fig.4(a)). The segmentation process was performed on the images added the Gaussian noise, which had the average zero, varying the standard deviation from 0 to 100. Fig.4(b) shows the image which is added Gaussian noise with the standard deviation 80 to Fig.4(a), and Fig.4(c) is the segment result of this image. Fig.4(d) shows the image which is added Gaussian noise with standard deviation 90 to Fig.4(a), and Fig.4(e) is the segmentation result of this image.

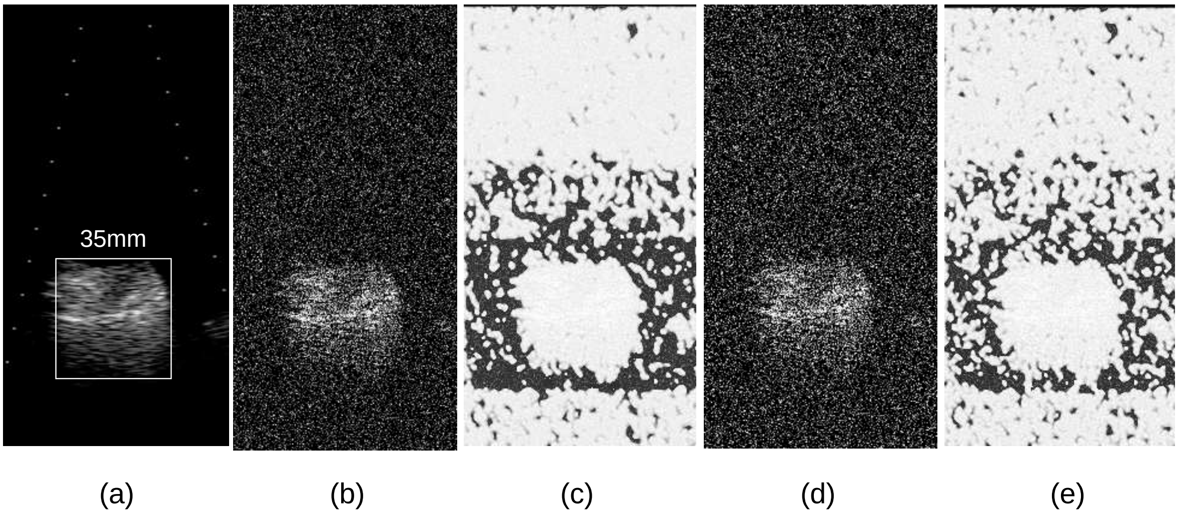

Figure 4: The image of meat cube cut off 35mm and fixed in a water tank. (a)The original image, (b)The image added the Gaussian noise with standard deviation 80 to (a), (c)The segmentation result of (b), (d)The image added the Gaussian noise with standard deviation 90 to (a), (e) The segmentation result of (d).

Fig.5 shows a correlation between the standard deviation of noise(σ) and the error rate of segmentation calculated by equation(3) shown in Fig.6. The segmentation error was fairly constant(about 10%) until $\sigma < 80$.

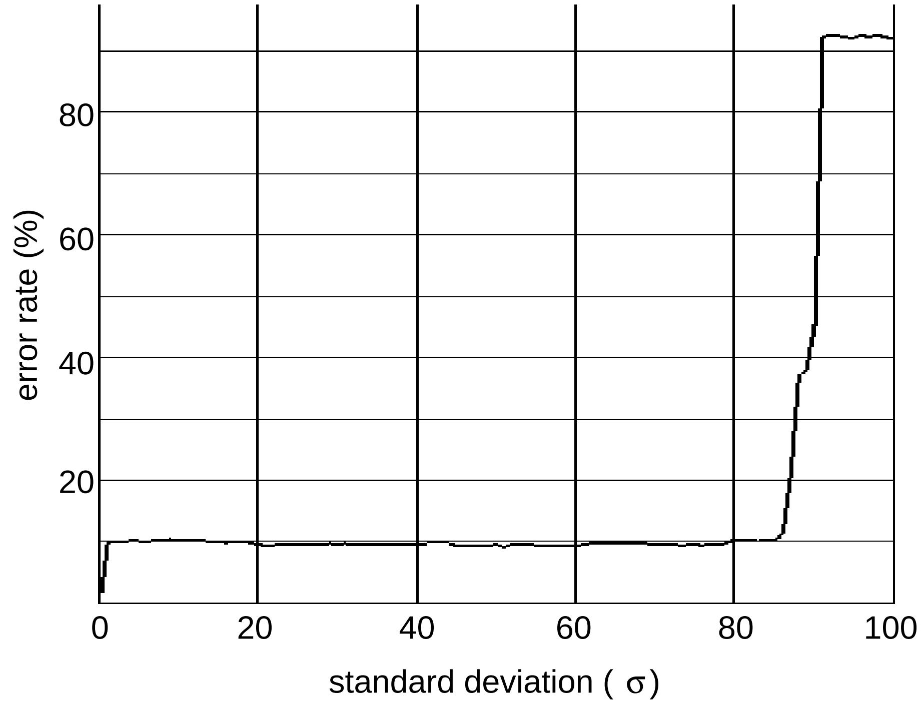

Figure 5: Correlation between error of segmentation and the noise.

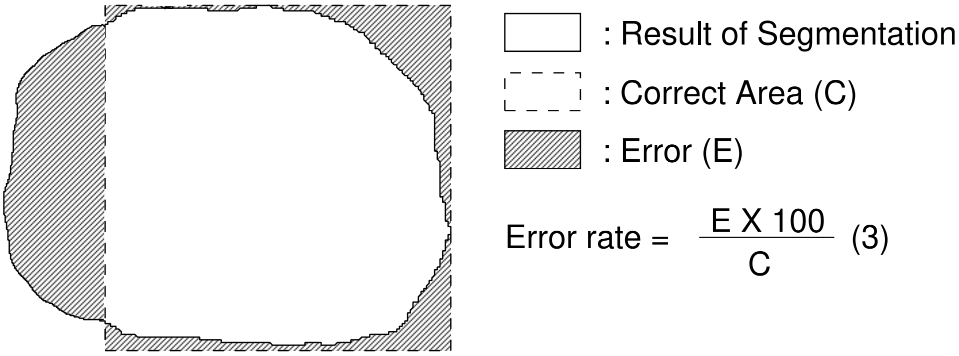

Figure 6: The method for the evaluation of the error rate of segmentation.

4.2 Accuracy of corresponding analysis

The accuracy of the corresponding analysis was evaluated using the 29 images of a bubble moving in a plastic pipe fixed in a water tank. The reason of using bubble is that its velocity is stable in the invariable flow of water and the form changes duaring its motion like a living organ. Fig.7 shows a part of the result of corresponding analysis. Blue indicates previous boundary, green indicates current boundary and red indicates the moving vector.

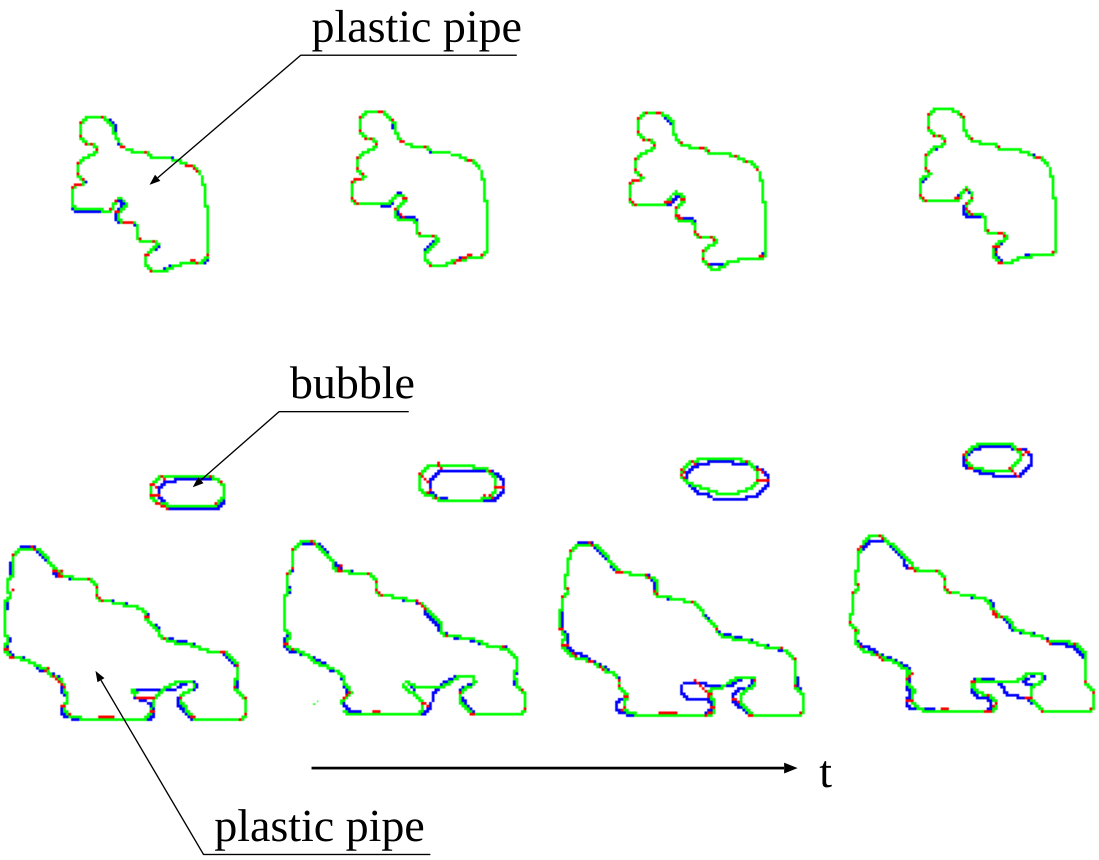

Figure 7: The result of corresponding analysis using moving bubble images.

Table.1 shows the true velocity of a bubble and the estimated one by our algorithm. The estimated value was the average of length of moving vector detected by this process, and true velocity was the number of pixels of a bubble in motion.

Table 1: True velocity of a bubble and estimated velocity in our algorithm.

	true value	estimated value	standard deviation
velocity(pixel/sec)	851	809	196

The true velocity is calculated by

$$v = D \times \frac{fr}{f} \tag{9}$$

where D is the distance of movement of bubble, fr is the frame rate and f is the number of frames using in this experiment. The estimated value has only 5% error.

4.3 Application for clinical images

We applied this technique for images in a short axis view. Fig.8 shows that transition velocity of the wall boundaries superimposed on B-mode echograms (Fig.1(a)) at a systolic phase with color classification. To normalize individual difference such as size of heart, the transition velocity is normalized as the ratio of a radius of a left ventricle to the transition distance. Red shows the part that the ratio of the transition to a radius of a left ventricle is less than 5%, blue is for 5-10% and green is for the rest. In general, it seems that the endocardial boundaries are smooth, then the detected boundaries are approximated with the cubic spline interpolation.

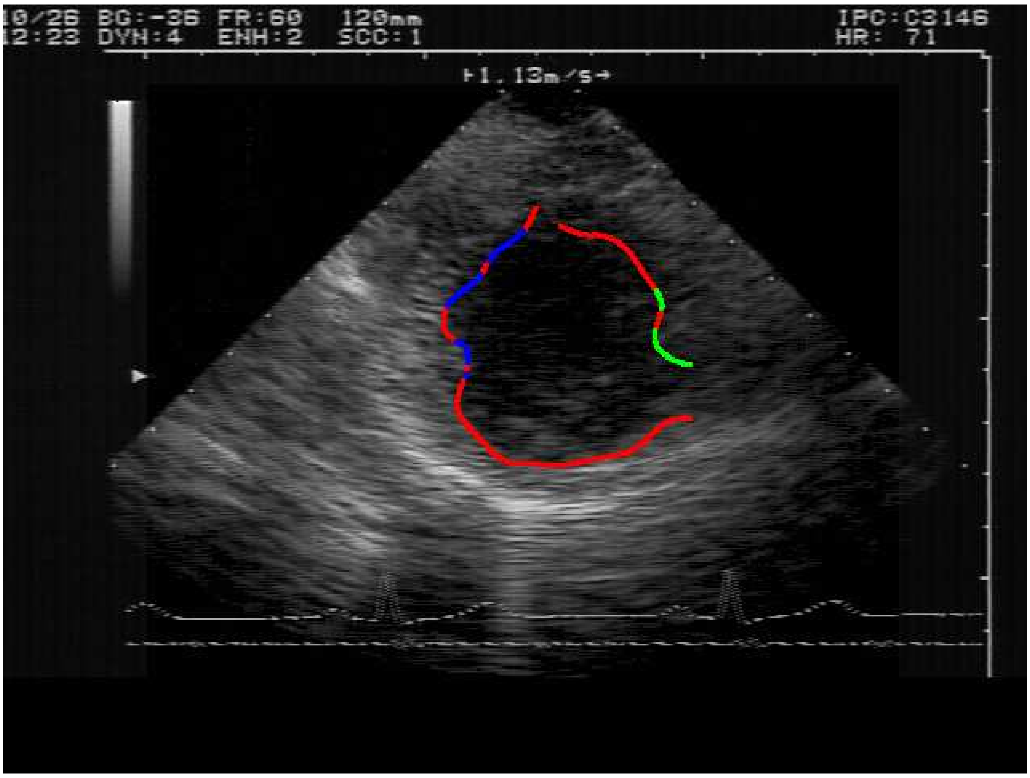

Figure 8: Transition velocity of the wall boundaries superimposed on B-mode image.

Fig.9 shows the time-velocity curve estimated at the same point for one cardiac cycle. Fig.9(a) is the case of a normal heart and (b) is that of a infarcted heart. In this graph, the velocity is normalized by the method mentioned above. When the wall goes away from the center of the left ventricle, the sign of velocity is indicated by plus. Otherwise, the sign of velocity is indicated by minus. It is obvious that the velocity of latter case is smaller than that of former case. A normal heart shows the maximum velocity more than 3 times as fast as the large of infarcted heart.

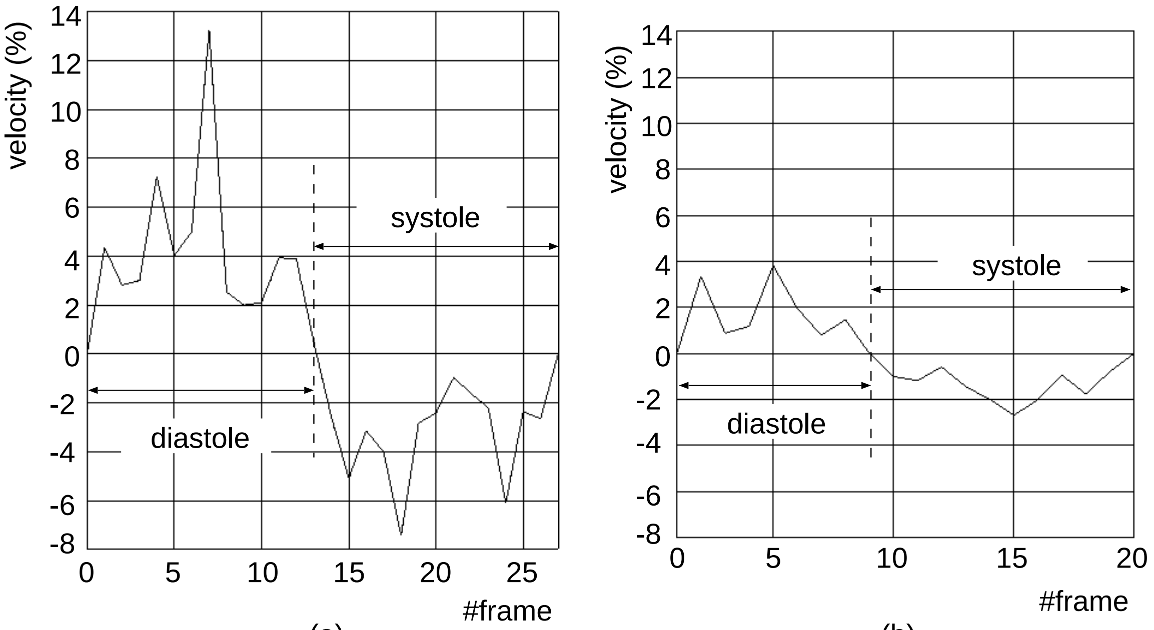

(a) (b)

Figure 9: The time-velocity curve measured for one cardiac cycle. (a)A normal heart, (b)An infarcted heart.

Examination of the processing time for this technique was carried out on the Sillicon Graphics ONYX Reality Engine^2. On average the segmentation and detection of landmarks required about 0.5sec an image and the correspondence analysis required about 0.56sec between successive frames.

5 Conclusions

In this paper, we examined the corresponding analysis of the landmarks obtained from the wall boundaries in a sequence of echocardiograms. The wall boundaries were obtained by segmentation using the gradient relaxation method and detection the contour. The landmarks were detected from these boundaries using its geometric features. Finally, landmarks were corresponded between two time-series echograms using the direction of edge and the moving distance, and the transition velocity could be obtained from the distance between corresponded landmarks. The transition velocity was normalized by a radius of a left ventricle and classified with colors and superimposed on the original image.

We evaluated the segmentation and the correspondence analysis method in vitro, then the accuracy of these methods was confirmed. Moreover the application for actual clinical images also was indicated.

Visualization of myocardial transition velocity allows quantitative evaluation of heart's function. Therefore, this technique is powerful tool for such aim.

References

[1] K.Masuda, K.Ishihara, T.Nagakura, T.Tsuda, T.Furukawa, H.Maeda, S.Kumagai and S.Kodama: Jpn. J. Appl. Phys., 33, (1994) pp.3134.

[2] N.Yamazaki, Y. Mine, A.Sano, M.Hirama, K.Miyatake, M.Yamagishi and N.Tanaka: Jpn. J. Appl. Phys., 33, (1994) pp.3141.

[3] 3) G.E.Mailloux, F.Langlois and P.Y.Simard: IEEE Trans. Med. Img., 8, (1989) pp.143.

[4] R.Muzzolini, Y.Yang and R.Pierson: IEEE Trans. Med. Img., 12, (1993) pp.108.

[5] B.Bhanu and O.D.Faugeras: IEEE Trans. Patt. Anal. and Mac. Intell., 3, (1982) pp.408.

[6] M.Yachida: Comp. Vision, Graphics, and Image Processing, 21, (1983) pp.262.

[7] G.S.Robinson: CGIP, 6, (1977) pp. 429.